

Critical behavior of single-crystal double perovskite $\text{Sr}_2\text{FeMoO}_6$

H. Yanagihara, Wesley Cheong, and M. B. Salamon

Department of Physics and Materials Research Laboratory, University of Illinois at Urbana-Champaign, Urbana, Illinois 61801

Sh. Xu

Department of Crystalline Materials Science, Nagoya University, Nagoya 464-8603, Japan

Y. Moritomo

CIRSE, Nagoya University, Nagoya 464-8601, Japan

(Received 1 September 2001; published 15 February 2002)

The critical behavior of the double perovskite $\text{Sr}_2\text{FeMoO}_6$ (SFMO) is investigated by measurements of the magnetization (M), susceptibility (χ), and temperature derivative of the resistivity ($d\rho/dT$), the last of which has the same critical exponent as the magnetic heat-capacity anomaly. The critical temperatures determined by both magnetization and $d\rho/dT$, are consistent and the critical exponents indicate that this material belongs to a three-dimensional Heisenberg ferromagnet universality class like such conventional metallic ferromagnets as Ni or Fe. We also show the existence of an extraordinary large magnetic resistivity temperate coefficient such as that of SrRuO_3 .

DOI: 10.1103/PhysRevB.65.092411

PACS number(s): 75.40.-s, 77.84.Bw

The double perovskite SFMO has one of the highest critical temperatures ($T_C \sim 410$ K) among half-metals, giving it great possibilities for applications. According to band calculations,¹ the majority band has a band gap and is mainly composed of Fe 3*d* states that are fully occupied ($S_{Fe} = 5/2$) while the Fermi level lies in a minority-spin band which is composed of mainly Mo 4*d* states ($S_{Mo} = 1/2$). Therefore, SFMO can be regarded as a mixed ferrimagnet, in that it has a localized spin 5/2 and an oppositely aligned itinerant spin 1/2. In addition to this unique electronic structure, the transport properties of single crystals and epitaxial films of SFMO show a metallic behavior, as expected from the band structure, but with a high residual resistivity at low temperatures and a much weaker temperature dependence than conventional ferromagnetic metals.²⁻⁵ In this sense, SFMO is quite an unusual magnetic material. In order to understand this unusual material better, we have investigated its critical behavior, expecting the universality class to which the material belongs to give important clues. We are motivated by the recent suggestions by Klein *et al.* that the critical behavior of the resistivity of SrRuO_3 , which does not appear to be that of conventional ferromagnetic metals, characterizes *bad* metallicity.⁶ In this paper, we find that the critical behavior of SFMO is close to that of Ni [a three-dimensional (3D) Heisenberg model] in spite of the half-metallic band structure and a mixed ferrimagnetism.

The SFMO single crystal was grown by the floating-zone method, the details of which can be found in Ref. 4. We measured magnetic properties via magnetization isotherms in magnetic fields up to 70 kOe from ~ 360 to ~ 450 K by using a commercial superconducting quantum interference device magnetometer. The mass of the sample was 7.3 mg, and we calculated the demagnetization factor ($4\pi N$) to be ~ 0.5 from its shape. The temperature at the sample position in the magnetometer was carefully corrected using a calibrated Pt thermometer which was also used for temperature-dependent resistivity measurements. The resistivity measure-

ments were performed by a dc four-probe technique, while slowly sweeping (typically 0.2 K/min) from room temperature to 480 K with a LakeShore 340 temperature controller. After smoothing over appropriate temperature intervals, the temperature derivative was taken. As a consequence, the $d\rho/dT$ curve obtained has an extrinsic rounding error (~ 0.2 K, $t \equiv |T - T_C|/T_C \sim 5 \times 10^{-4}$).

According to scaling laws, the spontaneous magnetization (M_S) and the initial susceptibility (χ_0) obey the following equations in the critical region:

$$M_S(T) = \lim_{H \rightarrow 0} M(H, T) \propto |T - T_{C-}|^\beta, T < T_C, \quad (1)$$

$$\chi_0^{-1}(T) = \lim_{H \rightarrow 0} H/M \propto |T - T_{C+}|^\gamma, T > T_C. \quad (2)$$

The typical procedure for extracting β and γ is to plot $M^{1/\beta}$ against $(H/M)^{1/\gamma}$, the so-called Arrott plots, and then to determine either $M_S(T)$ and $\chi_0^{-1}(T)$ by linearly extrapolating from a high-field region to both axes or by using a polynomial fit. In the case of our isothermal magnetization data sets, both M_S and χ_0^{-1} determined in this way are very sensitive to both the parameters of the Arrott plot and the extrapolation method. Since these critical exponents as well as T_C should be determined by some procedure as unequivocally as possible, we followed an iteration method recently used by Yang *et al.* for a critical behavior analysis of CrO_2 films.⁷ Starting from some plausible combination of β and γ (~ 0.370 and ~ 1.33 , respectively) as the initial values, we determine $M_S(T)$ and $\chi_0(T)$ by a linear extrapolation to both axes, and then obtain β , γ , and $T_{C\pm}$, by fitting with Eqs. (1) and (2). We continue this procedure using the obtained exponents as initial guesses until both initial and final exponents become consistent, and the difference between T_{C-} and T_{C+} becomes negligible. The Arrott plot of the isothermal data sets from 362.58 to 448.09 K, with $\beta = 0.385$ and

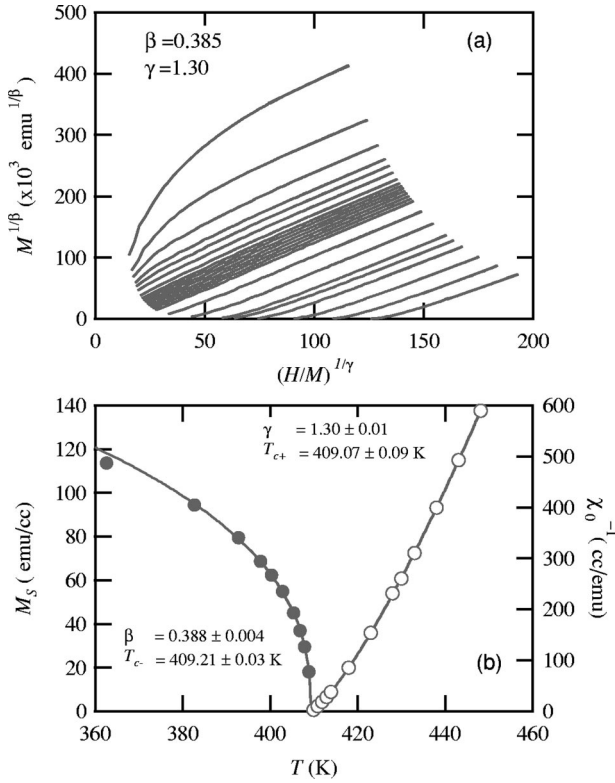


FIG. 1. Top panel (a): the isotherms of $M^{1/\beta}$ vs $(H/M)^{1/\gamma}$ (the Arrott plot). The curves near T_C are quite straight, implying that both plot parameters β and γ are reliable values. Here, $\beta=0.385$ and $\gamma=1.30$. Bottom panel (b): the plot of M_S (closed circles) and χ_0^{-1} (open circles) vs T . M_S and χ_0^{-1} are determined by a linear extrapolation of the Arrott plot (see the text). Solid lines are fit curves for Eqs. (1) and (2).

$\gamma=1.30$ is shown in Fig. 1(a). Although these critical exponents must ideally converge to some combination of values after a number of iterations, there are always differences between the initial and final exponents, and the process does not seem to converge to some values. Therefore, our criterion is to stop the iteration process when the initial values are within the error bars of the final fit results. The temperature dependence of obtained $M_S(T)$ and $\chi_0^{-1}(T)$ are displayed in Fig. 1(b). The fit parameters β and γ , finally obtained, are 0.388 ± 0.004 and 1.30 ± 0.01 , respectively. The determined T_C 's for both scaling equations are $T_{C-} = 409.21 \pm 0.03$ K and $T_{C+} = 409.07 \pm 0.09$ K, respectively and they are very

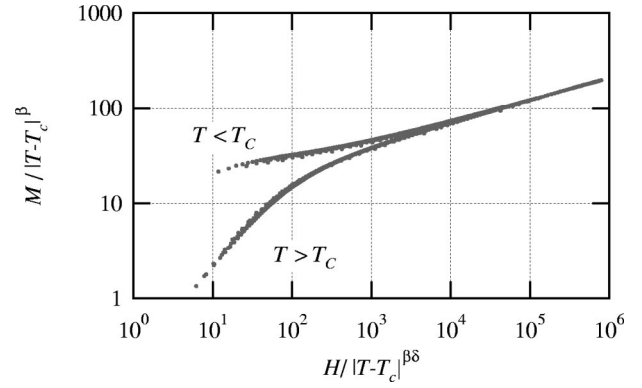


FIG. 2. $M/|T-T_C|^\beta$ vs $H/|T-T_C|^{\beta\delta}$ plot of SFMO, using $\beta=0.388$, $\delta=(\beta+\gamma)/\beta=4.35$, and $T_C=409.1$ K.

close to each other. The M_S data point at 362.58 K is slightly below the fitted curve, which might suggest that this temperature is out of the critical region. The value β is slightly larger than that of the 3D Heisenberg model, but close to that of Ni.⁸ Also, γ is very close to that of Ni (Ref. 8) (cf. Table I). In order to judge the validity of this analysis and to confirm better the obtained critical exponents and T_C , we performed another scaling test. The scaling laws predict that the magnetization satisfies the equation

$$M(T)/|T-T_C|^\beta = f(H/|T-T_C|^{\beta\delta}). \quad (3)$$

Here $f(x)$ is an unknown function. Using the scaling relation $\delta=(\beta+\gamma)/\beta$,⁹ we can easily confirm the relation between normalized M and normalized H with β and γ (Fig. 2) obtained above. A T_C of 409.1 K was tentatively selected as an intermediate value between $T_{C\pm}$; however, such a small deviation of T_C has little effect on data collapse. As seen in Fig. 2, all the data fall on two universal curves, this scaling behavior strongly suggesting that our estimation procedure and the values for β , γ , and T_C are quite reliable. $\delta=4.35$ is indeed close to that of Ni,⁸ because of the consistency of scaling laws. The critical exponents of SFMO obtained in this study are listed in Table I along with those of some other ferromagnets and of theoretical models for comparison. One may note that one of the two curves at low field, far from T_C for $T < T_C$ shows a slight downturn rather than being flat. We believe the reason for this is mainly an effect of magneto-crystalline anisotropy, because, when taking the magnetization data, the magnetic easy axis of the sample was not per-

TABLE I. Critical parameters of SFMO, conventional ferromagnetic metals, and 3D Heisenberg models for comparison.

Materials	T_C (K)	α	β	γ	δ	Ref.
3D Heisenberg		-0.12	0.365	1.39	4.80	
Ni	635.5		0.379~0.405	1.34	4.35	8
	~631.58	-0.10				10
CrO ₂	386.50		0.371	1.43	4.85	7
SrRuO ₃	~150	~-1 ($T > T_C$)	0.325	1.38		6
SFMO	409.1(409.9 ^a)	-0.12 ^a	0.388	1.30	4.35	present work

^aDeduced from the dp/dT anomaly (see the text).

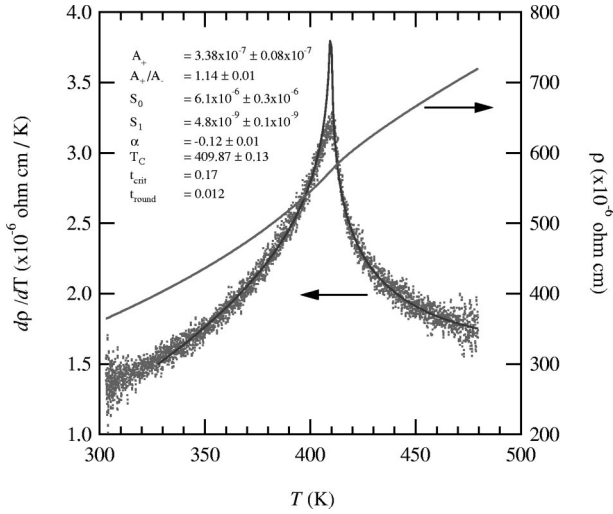


FIG. 3. $\rho-T$ and $d\rho/dT$ plots near T_C . The resistivity shows a kink near T_C , and is metallic even above T_C . Fit results are also shown on $d\rho/dT$ plots (see the text).

fectly aligned with the magnetic-field direction. The magnetic anisotropy abruptly decreases with increasing temperature to T_C and therefore this effect could be negligible near and above T_C and at high field. However, it might cause a significant deviation from the ideal curves much below T_C , especially at low field.

We now turn to the critical behavior of the resistivity. In Fig. 3, the temperature-dependent resistivity and its derivative near T_C are shown. In contrast to the $\rho-T$ curves of the polycrystalline samples,¹ the curve of the single-crystal sample shows a metallic behavior over the entire measured temperature regime. $d\rho/dT$ shows a strong cusp at T_C , similar to that of a specific-heat anomaly. In the case of conventional ferromagnetic metals, $d\rho/dT$ curves are proportional to specific-heat curves in the critical region; in other words, the critical exponent of $d\rho/dT$ is the same as α , the critical exponent of specific heat.^{11–14} Therefore, assuming this relation to hold, it is possible to obtain the critical exponent α by applying the same analysis as for the critical behavior of the heat capacity¹⁵ to $d\rho/dT$ curves, that is,

$$d\rho/dT = (A_{\pm}/\alpha) |(T - T_C)/T_C|^{-\alpha} + S_0 + S_1(T - T_C). \quad (4)$$

Here, $+$ ($-$) refer $T > T_C$ ($T < T_C$), and S_0 and S_1 are approximations of the nonmagnetic temperature coefficients of resistance. As in many materials, we assume that $\alpha = \alpha'$; that is, the critical exponents for $T > T_C$ and $T < T_C$ are identical. Because of either intrinsic¹⁶ or experimental rounding effects near T_C , the data points $T_C \pm \sim 5$ K ($t_{round} \leq 10^{-2}$) were excluded. We considered the $T_C \pm 70$ K ($t_{crit} \leq 0.17$) data points to be in the critical region; however, the range did not affect the fit results so much. The best-fit result is also shown in Fig. 3. The results of α and the amplitude ratio A_+/A_- are -0.12 ± 0.01 and 1.14 ± 0.01 , respectively. There is a slight discrepancy between the obtained $T_C = 409.87 \pm 0.13$ and those of M_S and χ_0^{-1} scalings, probably due to the tem-

perature correction error. The values obtained are very close to those of a conventional ferromagnet such as Ni (Ref. 10) or Fe,¹⁴ and satisfy the scaling relation; $\alpha + 2\beta + \gamma = 2$ within a reasonable error. Furthermore, the fact that the critical behavior of $d\rho/dT$ can be described by the Fisher-Langer picture indicates that the electronic structure does not change abruptly above and below T_C .

We also need to comment on the differences between a ferromagnet and a ferrimagnet in terms of critical behavior. It is known that a ferrimagnet shows the same scaling laws, such as Eqs. (1)–(3), with exponents similar to those of conventional ferromagnets¹⁷ despite their more complicated spin structures. Indeed, in the case of SFMO, it seems more like a ferromagnet¹⁸ than a typical ferrimagnet with two sublattices. In fact, a recent experiment revealed that the magnitudes of the Mo moments, presumably coupled to localized Fe moments, are negligibly small;¹⁹ therefore, the two-sublattice ferrimagnetic picture may not be appropriate.

Although the absolute value of $d\rho_M/dT$ near T_C is quite large for SFMO, even a few times larger than for SrRuO₃ [cf. Fig. 3(a) in Ref. 6], we should take account the ratio of $d\rho_M/dT$ at T_C to ρ_{MAG} , which is the incoherent spin resistivity at high temperature [$\rho_M(T \gg T_C)$], and which should be saturated at this temperature regime. In order to estimate ρ_{MAG} empirically, we assume that the main contribution of the resistivity is decomposed into the residual resistivity ρ_0 , a magnetic scattering term $\rho_M(T)$, and a lattice scattering term with a Bloch-Grüneisen form $\rho_{latt}(T)$,²⁰ that is, $\rho(T) = \rho_0 + \rho_M(T) + \rho_{latt}(T)$. Here ρ_{latt} is a function that increases as T^5 at low temperature, and as T above the Debye temperature Θ_D . In the case of conventional ferromagnetic metals above both T_C and Θ_D , ρ_{MAG} is independent of T , and $d\rho/dT$ is solely proportional to $A/4\Theta_D$. By substituting Θ_D of ~ 397 K determined by the low-temperature heat-capacity data,² the coefficient A can be determined. However, the resulting ρ_{MAG} is problematic; ρ_{latt} estimated in this way is far larger than the measured total ρ at some temperature regime, suggesting that our $\rho_{latt}(T)$ is overestimated in this analysis, and that some magnetic scattering contribution remains even above both T_C and Θ_D . It is possible that the high-temperature region, where we assumed that only the electron-phonon scattering contributes to $d\rho/dT$, is still within the critical regime, and therefore that $\rho_M(T)$ is still varying in this regime.

As an alternative way to estimate ρ_{MAG} , we can directly calculate it by adopting Kasuya's model²¹ for high-temperature ρ_{MAG} , namely, $\rho_{MAG} = (3\pi m^*/Ne^2\hbar^2)S(S+1)J_{c-d}^2/E_F$, where m^* , S , J_{c-d} , and E_F are the effective mass of conduction electrons, the spin number of the localized electron ($S = 5/2$ for the present case), the exchange coupling strength between spins of the conduction electron and localized spins, and the Fermi energy, respectively. Substituting the thermal effective mass ($m^*/m \sim 3.3$) from the low-temperature electron heat capacity,² the coupling constant ($J_{c-d} = -18$ meV),²² and free-electron values for those not reported into the above equation, we obtain $\rho_{MAG} \approx 230 \mu\Omega$ cm. The result is that $1/\rho_{MAG} d\rho_M/dT$ is

TABLE II. Resistivity anomaly parameters of different materials.

Materials	$d\rho_M/dT$ $\mu\Omega$ cm/K	ρ_{MAG} $\mu\Omega$ cm	$1/\rho_{MAG}d\rho_M/dT$ $\times 10^{-3}$ K $^{-1}$	Ref.
Ni	0.11	15	7.3	23 and 20
Fe	0.26	80	3.3	14 and 20
SrRuO ₃	1.2	80	15.0	6
SFMO	2	230	8.7	present work

8.7×10^{-3} K $^{-1}$, comparable to that of SrRuO₃ ($\sim 1.5 \times 10^{-2}$ K $^{-1}$). As shown in Table II for comparison, the $1/\rho_{MAG}d\rho_M/dT$ of SrRuO₂ is apparently larger than that of Fe, but is only twice as large as that of Ni, which is also a conventional ferromagnet. Therefore, it seems hard to conclude that there is a relation between the amplitude of $1/\rho_{MAG}d\rho_M/dT$ and the classification of ferromagnetic metals.

Despite normalization by the incoherent scattering, $(d\rho/dT)_{crit}$ is several times larger than that of conventional ferromagnets, and may be intimately related to its unique electronic structure. Furthermore, it may suggest a connection to the breakdown of the Boltzmann picture in this system, similar to the anomaly of SrRuO₃.⁶ However, unlike SrRuO₃, SFMO does not show any discrepancy in terms of the critical behavior as a ferromagnetic metal, including the electrical resistivity anomaly and the scaling relations between α , β , and γ , as we showed above. Our method to estimate the above ρ_{MAG} may be too oversimplified; therefore, the $1/\rho_{MAG}d\rho/dt$ may not be so large compared with conventional one. In order to make this argument experimentally clearer, higher-temperature resistivity measurements are needed.

This material was based upon work supported in part by the U.S. Department of Energy, Division of Materials Sciences under Award No. DEFG02-91ER45439, through the Frederick Seitz Materials Research Laboratory at the University of Illinois at Urbana-Champaign.

-
- ¹K.-I. Kobayashi, T. Kimura, H. Sawada, K. Terakura, and Y. Tokura, *Nature* (London) **395**, 677 (1998).
²Y. Tomioka, T. Okuda, Y. Okimoto, R. Kumai, K.-I. Kobayashi, and Y. Tokura, *Phys. Rev. B* **61**, 422 (2000).
³W. Westerburg, D. Reisinger, and G. Jakob, *Phys. Rev. B* **62**, 767 (2000).
⁴Y. Moritomo, S. Xu, A. Machida, T. Akimoto, E. Nishibori, M. Takata, M. Sakata, and K. Ohyama, *J. Phys. Soc. Jpn.* **69**, 1723 (2000).
⁵H. Yanagihara, M. B. Salamon, Y. Lynda-Geller, S. Xu, and Y. Moritomo, *Phys. Rev. B* **64**, 214407 (2001).
⁶L. Klein, J. S. Dodge, C. H. Ahn, G. J. Snyder, T. H. Geballe, M. R. Beasley, and A. Kapitulnik, *Phys. Rev. Lett.* **77**, 2774 (1996); R. Roussev and A. J. Millis, *ibid.* **84**, 2279 (2000).
⁷F. Y. Yang, C. L. Chien, X. W. Li, Gang Xiao, and A. Gupta, *Phys. Rev. B* **63**, 092403 (2001).
⁸M. Seeger, S. N. Kaul, H. Kronmüller, and R. Reisser, *Phys. Rev. B* **51**, 12 585 (1995).
⁹H. Eugene Stanley, *Introduction to Phase Transition and Critical Phenomena* (Oxford University Press, New York, 1971).
¹⁰D. L. Connelly, J. S. Loomis, and D. E. Mapother, *Phys. Rev. B* **3**, 924 (1971).
¹¹M. E. Fisher and J. S. Langer, *Phys. Rev. Lett.* **20**, 665 (1968).
¹²S. Alexander, J. S. Helman, and I. Balberg, *Phys. Rev. B* **13**, 304 (1976).
¹³D. S. Simons and M. B. Salamon, *Phys. Rev. B* **10**, 4680 (1974).
¹⁴L. W. Shacklette, *Phys. Rev. B* **9**, 3789 (1974).
¹⁵A. Kornblit and G. Ahlers, *Phys. Rev. B* **11**, 2678 (1975).
¹⁶One may wonder why the rounding effect is so large. Since the single crystal SFMO contains only a few ($\sim 10\%$ in this case,) antisite defects which are substitution defects between Fe and Mo ions (see Refs. 2 and 4), such defects could be an origin of the rounding.
¹⁷K. Ohbayashi and S. Iida, *J. Phys. Soc. Jpn.* **25**, 1187 (1968); S. Freeman and P. Wojtowicz, *Phys. Rev.* **177**, 882 (1969); R. G. Bowers and B. Y. Yousif, *Phys. Lett.* **96A**, 49 (1983).
¹⁸High-temperature susceptibility data imply that this material is not a conventional ferrimagnet but rather a ferromagnet, because the paramagnetic Curie temperature is positive and the Curie constant is close to that of $S=4/2$, and not the sum of the two components of both S_{Fe} and S_{Mo} .
¹⁹Sugata Ray, Ashwani Kumar, D. D. Sarma, R. Cimino, S. Turchini, S. Zennaro, and N. Zema, *Phys. Rev. Lett.* **87**, 097204 (2001).
²⁰R. J. Weiss and A. S. Marotta, *J. Phys. Chem. Solids* **9**, 302 (1959).
²¹T. Kasuya, *Prog. Theor. Phys.* **16**, 58 (1956).
²²D. D. Sarma, P. Mahadevan, T. Saha-Dasgupta, S. Ray, and A. Kumar, *Phys. Rev. Lett.* **85**, 2549 (2000).
²³F. C. Zumsteg and R. D. Parks, *Phys. Rev. Lett.* **24**, 520 (1970).